IEEE Photonics Journal
An IEEE Photonics Society Publication

Open Access

The Effect of Chirp on Pulse Compression at a Group Velocity Horizon

Volume 8, Number 3, June 2016

Ihar Babushkin
Shalva Amiranashvili
Carsten Brée
Uwe Morgner
Günter Steinmeyer
Ayhan Demircan

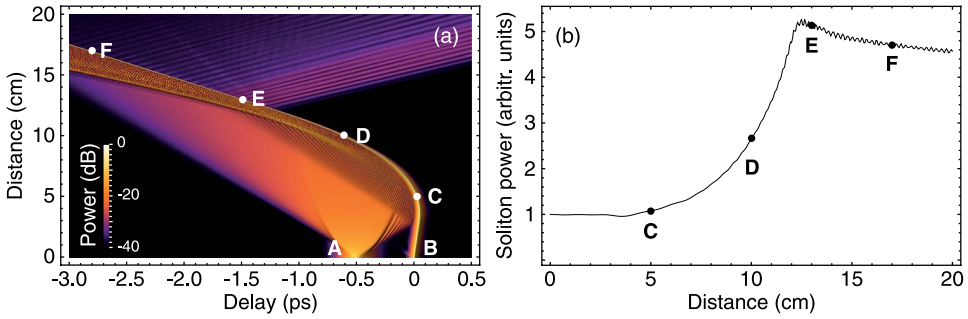

DOI: 10.1109/JPHOT.2016.2570001
1943-0655

The Effect of Chirp on Pulse Compression at a Group Velocity Horizon

Ihar Babushkin,[1,2] Shalva Amiranashvili,[3] Carsten Brée,[3] Uwe Morgner,[1,4] Günter Steinmeyer,[2] and Ayhan Demircan[1,4]

[1]Institute for Quantum Optics, Leibniz Universität Hannover, 30167 Hannover, Germany
[2]Max Born Institute, 12489 Berlin, Germany
[3]Weierstrass Institute for Applied Analysis and Stochastics (WIAS), 10117 Berlin, Germany
[4]Hannover Centre for Optical Technologies, 30167 Hannover, Germany

DOI: 10.1109/JPHOT.2016.2570001

Manuscript received April 20, 2016; accepted May 14, 2016. Date of publication May 17, 2016; date of current version June 6, 2016. This work was supported by the Einstein Center for Mathematics Berlin under Project D-OT2, by the German Research Foundation (DFG) under Projects BA 4156/4-1 and MO 850/19-1, by the Nieders Vorab under Project ZN3061. Corresponding author: I. Babushkin (e-mail: ihar.babushkin@gmail.com).

Abstract: Group-velocity matched cross-phase modulation between a fundamental soliton and a dispersive wave packet has been previously suggested for optical switching applications similar to an optical transistor. Moreover, the nonlinear interaction in the resulting group-velocity horizon can be exploited for adiabatic compression of the soliton down into the few-cycle regime. Here, we study the delicate phase- and frequency-matching mechanism of soliton/dispersive wave interaction by controlling the input chirp of the dispersive wave. We demonstrate that such a modification of the dispersive wave can significantly alter the soliton dynamics. In particular, we show that it allows a decrease of the fiber length needed for the best compression and, to some extent, control of the trajectory of the soliton. The mechanism of such an influence is related to the modification of the phase-matching condition between the soliton and dispersive wave.

Index Terms: Pulse compression, waveguides, ultrafast optics, chirp.

1. Introduction

The study and generation of light pulses that encompass only a few cycles of the electric field is a major topic in ultrafast optics, and nowadays, ultrashort pulses can be generated in a wide spectral range. Different technologies, such as chirped pulse amplification, filament self-compression, or optical parametric amplification, provide nearly single-cycle pulses from the ultraviolet to the THz regime. While Ti:sapphire and its harmonics conveniently offer fairly direct schemes toward ultrashort pulses from the near infrared well into the ultraviolet, the mid-infrared (wavelength 2–25 μm) is a notoriously challenging range for direct laser-based schemes. Optical parametric schemes offer a convenient alternative, but require carefully designed phase-matching ranges and are difficult to implement. Another alternative is use of gas-filled hollow core crystal fibers [1].

A recently suggested new scheme [2], which is discussed in what follows, relies on cross-phase modulation (XPM) between two group-velocity matched pulses at different wavelengths. The matching condition is automatically met in fibers/materials in the vicinity of the

zero dispersion wavelength (ZDW), where the group velocity reaches its maximum (minimum) value. A soliton with the carrier frequency in the negative group velocity dispersion (GVD) domain may then co-propagate with the dispersive pulse in the positive GVD domain such that both pulses have nearly equal velocities and considerably different wavelengths.

The key point is that a short intense soliton yields a noticeable nonlinear change of the refractive index, a kind of a moving barrier or a "mirror" for the second usually weaker pulse. The refractive index barrier manifests itself via XPM effect that modifies velocity of the second pulse. Numerical solutions suggest that the soliton and the dispersive pulse became temporally locked to each other. This process will be referred to as *collision of pulses*. The collision may alternatively be understood as *scattering or reflection* of the dispersive radiation at the refractive index barrier created by the soliton [3]–[5]. These kinds of XPM interactions are known as the optical *push broom* effect [6], and there is a noteworthy analogy to the so-called *optical event horizon*, see [7], [8]. Similar interactions can be found in other nonlinear wave systems, e.g., in fluid dynamics [9]. In the optical context, dispersive waves scattered on solitons naturally appear in supercontinuum generation by soliton fission [10]–[12]; moreover, the standard fundamental soliton can be replaced by a higher order soliton or even by a dark soliton [13], [14]. Direct experimental verification of the reflection process at the soliton-induced refractive index barrier can be found in [7] and [15]–[18].

The above cited numerical simulations indicate that the velocity-matched XPM interaction may yield sufficient changes of both pulses. In the first place, reflection on a moving refractive barrier changes carrier frequency of the dispersive pulse [5]. Due to energy conservation, the change induces a less pronounced frequency shift of the soliton. The shift becomes especially important if the GVD value experienced by the soliton depends on frequency in a sharp manner. An induced change of the GVD parameter enables soliton manipulation by a much weaker dispersive pulse [2], [17], [19]–[22]. Among other things, soliton compression and generation of few-cycle pulses becomes possible by blue shift of the soliton [23]. Very recently, this novel type of soliton compression was experimentally demonstrated [24] with pulse durations that seem to be far from exploiting the full potential of the method. This experimental verification employed two coherent pulses at $\approx$ 600 and 800 nm and a fiber with zero-dispersion wavelength at $\approx$ 700 nm.

On the other hand, the compression scheme, as suggested in [23] and released in [24], has its practical limitations. Given both a certain fiber GVD profile and a certain soliton to compress, one has to employ a group velocity matched second pulse. The carrier frequency of the second pulse is then prescribed and we are left with its duration/amplitude and with the initial delay between the pulses as possible control parameters. Note that use of longer dispersive pulses seems to be impractical, because the compressed soliton quickly changes its carrier frequency thus destroying the velocity matching condition. The situation is even more unfortunate in the presence of the soliton self-frequency shift due to Raman effect. If the initial delay is too large, the soliton has enough time to change its carrier frequency before the collision, and thereafter, the velocity matching condition breaks down and diminishes soliton compression.

In the present article we introduce one additional control parameter, namely we investigate the influence of the chirp in the dispersive pulse. An extraneous possibility to manage pulses is welcome, the more so because in practice all pulses are chirped to some extent and one should know what chirp values can be tolerated without preventing compression. Note, that on one hand the imposed chirp modifies pulse frequency, which also modifies the interaction "strength" between the chirped dispersive pulse and the soliton. On the other hand, the chirped pulse self-consistently reshapes due to dispersion. We show that both effects play a noticeable role and may be used as a mean to control the trajectory of the soliton, as well as compression dynamics.

2. Adjustable Pulse Compression at a Group-Velocity Horizon

We consider plane-polarized electromagnetic waves that propagate in a 1-D setting. In the simplest case of bulk propagation, the wave may be completely characterized by its field

$E(z,t)$, and in a more complex case of a polarization-preserving optical fiber, $E(z,t)$ refers to the amplitude of the relevant fiber mode. To model collision and scattering of two co-propagating pulses with considerably different carrier frequencies, we split the field $E(z,t)=\int_{-\infty}^{\infty}\widetilde{E}(z,\omega)e^{-i\omega t}(d\omega/2\pi)$ into negative-and positive-frequency parts $E=E_-+E_+$, where

$$E_-(z,t)=\int_{-\infty}^{0}\widetilde{E}(z,\omega)e^{-i\omega t}\frac{d\omega}{2\pi},\qquad E_+(z,t)=\int_{0}^{\infty}\widetilde{E}(z,\omega)e^{-i\omega t}\frac{d\omega}{2\pi}$$

and describe the field in terms of the so-called analytic signal $\mathcal{E}(z,t)=2E_+(z,t)$. Note that $E(z,t)=\mathrm{Re}[\mathcal{E}(z,t)]$ is real-valued and contains both positive and negative frequencies, whereas $\mathcal{E}(z,t)$ is complex-valued, contains only positive frequencies, and is defined without any reference to the pulse carrier frequency and slowly varying envelope approximation [25], [26]. The complex field is subject to a bidirectional propagation equation [27]; in what follows, we will use its unidirectional version

$$\partial_z\mathcal{E}+\hat{\beta}\mathcal{E}+\frac{n_2}{c}\partial_t\left(f_K|\mathcal{E}|^2\mathcal{E}+f_R\mathcal{E}\hat{h}|\mathcal{E}|^2\right)_+=0 \tag{1}$$

where we assume a cubic (Kerr) nonlinearity.

Equation (1), in which n_2 is the nonlinear refractive index and c the speed of light, is similar to the generalized nonlinear Schrödinger equation (GNLSE, see [28]). The only structural difference is that the negative-frequency part of the nonlinear terms like $|\mathcal{E}|^2\mathcal{E}$ is put to zero, this is indicated by the notation $(|\mathcal{E}|^2\mathcal{E})_+$. The operator $\hat{\beta}$ is defined in the frequency domain by the propagation constant $\beta(\omega)$, such that $\hat{\beta}e^{-i\omega t}=-i\beta(\omega)e^{-i\omega t}$. Therefore for a linear wave with $\mathcal{E}\sim e^{ikz-i\omega t}$ (1) naturally yields $k=\beta(\omega)$. Note that fiber modes do not exist for all frequencies, the same applies to $\beta(\omega)$. Fortunately, the problem does not affect our calculations as long as both the soliton and the dispersive wave are well separated from the cut-off frequency. Note also that (1) ignores the backward waves that are permanently generated by the nonlinear term, this is possible as long as $n_2|\mathcal{E}|^2\ll 1$; see [29] and [30]. Equation (1) is different from the known unidirectional pulse propagation equation [31]–[34] by neglecting the terms like $\mathcal{E}^3$.

The parameters f_K and $f_R=1-f_K$ describe relative contributions of the Kerr and Raman effect, respectively, and $\hat{h}$ denotes a standard convolution with the Raman response function

$$\hat{h}|\mathcal{E}(z,t)|^2=\int_0^{\infty}h(t')|\mathcal{E}(z,t-t')|^2dt',\qquad h(t')=\frac{\tau_1^2+\tau_2^2}{\tau_1\tau_2^2}e^{-t'/\tau_2}\sin\left(\frac{t'}{\tau_1}\right).$$

As a nonlinear dispersive medium we exemplarily choose an endlessly single-mode (ESM) photonic crystal fiber [35]. The expression for $\beta(\omega)$ and the specific values of $f_{K,R}$ and $\tau_{1,2}$ are specified in [23]. We neglect a frequency dependence of n_2. It is convenient to solve (1) in the moving frame replacing the laboratory time t by the delay $\tau=t-z/V$ and $\beta(\omega)$ by $\beta(\omega)-\omega/V$. The velocity V of the moving frame is chosen to be the common velocity of the velocity matched pulses. For numerical solution we use a de-aliased pseudo-spectral method, with the implementation of the Rung–Kutta integration scheme in the frequency domain and adaptive step-size control. The quality of the time discretization is ensured by exemplary runs with a considerably larger number of harmonics.

This approach addresses the interaction of two pulses at well-separated carrier frequencies away from restrictions of the slowly-varying envelope approximation. The carrier frequencies may be separated by an octave or more, as we are interested in a fundamental soliton in the mid-IR and a dispersive wave close to the ultraviolet region. We note in this respect that pulse compression in all calculations that are described in what follows occurs on a space interval of only a few centimeters of propagation length. Therefore, the absorption, which is less than

0.1 dB/m in the whole spectral region under consideration is unlikely to affect the compression as such. In turn, the absorption shall continuously decrease the peak intensity as the already compressed soliton propagates further along the fiber.

In terms of choice of the medium, we only require a dispersion profile with at least one ZDW. Such a precondition is given in a large class of silica-based fibers, but also in other materials as, e.g., fluoride based ZBLAN fibers [36]. Moreover, adequate dispersion profiles can be found in Raman-free gas-filled hollow core Kagome photonic crystal fibers [1], where the dispersion properties can additionally be adjusted by pressure variation. The Kagome fibers can be used for self-compression of optical pulses to a single-cycle regime [1]. As to the chosen ESM fiber, anomalous and normal dispersion branches are shown in Fig. 2(a) and (b), together with a suitable group-velocity matched frequency combination (red and blue points for the soliton and dispersive wave respectively) shown for the GVD in Fig. 2(a) and (b) and for the group index in Fig. 3(a).

For our pulse compression scheme, we inject two pulses: soliton $\mathcal{E}_s$ at frequency ω_s and dispersive wave $\mathcal{E}_d$ at frequency ω_d on both sides of the ZDW

$$\mathcal{E}(z,t)|_{z=0} = \mathcal{E}_s(t) + \mathcal{E}_d(t)$$

$$\mathcal{E}_s(t) = \frac{\mathcal{E}_{s0}}{\cosh\left(\frac{t}{t_s}\right)} e^{-i\omega_s t}, \qquad \mathcal{E}_d(t) = \mathcal{E}_{d0} \exp\left[-\frac{1+iC}{2}\frac{(t+t_0)^2}{t_d^2}\right] e^{-i\omega_d t},$$

such that $\beta'(\omega_s) = \beta'(\omega_d)$. We use the following parameters

$$\begin{array}{llll} \sqrt{n_2}\mathcal{E}_{s0} = 0.0173, & t_s = 16.7\,\text{fs}, & \lambda_s = 2200\,\text{nm}, & \\ \sqrt{n_2}\mathcal{E}_{d0} = 0.0122, & t_d = 62.5\,\text{fs}, & \lambda_d = 542\,\text{nm}, & t_0 = 500\,\text{fs} \end{array} \tag{2}$$

where the value of $\mathcal{E}_{s0}$ corresponds to the exact fundamental soliton of the nonlinear Schrödinger equation for the (negative) GVD $\beta''(\omega_s)$. Compared to the previous work [23], we additionally introduce the possibility of a variable initial linear chirp in the dispersive wave, determined by the dimensionless parameter C. We note that for generic pulse shapes, there is no simple and generally valid relation between C and the group delay dispersion (GDD). Assuming Gaussian pulse shapes, one can relate GDD by calculating the distance required to fully compensate the chirp in the medium via $\beta''(\omega_d)$; then, GDD $= -t_d^2 C/(1+C^2)$.

As an introductory example, we consider a Raman-free fiber and an unchirped dispersive wave $(C = 0)$. Figs. 1 and 2 display the scattering of the dispersive wave on the fundamental soliton in the space-time and spectral domains, respectively. When parts of the dispersive wave reach the edge of the soliton [see the CDE curve in Fig. 1(a)], frequency shifts of both the soliton and the reflected dispersive wave are induced. In our set-up the dispersive wave is injected earlier into the fiber, so that a collision occurs at the leading edge of the soliton. This process results in a blue-shift of the soliton center frequency [see Fig. 2(a) and (c)] and a stronger red-shift of the dispersive wave [see Fig. 2(b) and (d)]. Eventually, the entire spectrum of the dispersive wave is depleted and nearly all frequencies are converted to the range of 370 to 460 THz. Simultaneously, the soliton frequency is up-shifted from 136 to 170 THz. The latter process is accompanied by soliton compression [see Fig. 1(b)] and spectral broadening from about 40 THz to more than 100 THz [see Fig. 2(c)]. These frequency shifts automatically lead to a change of the GVD [see arrows in Fig. 2(a) and (b)] and, of course, the group velocity as such. In this example, both pulses are shifted toward the larger group velocity [see Fig. 3(a)].

Enabling longer interaction zones of the soliton and parts of dispersive waves, a concomitant acceleration of the soliton may be achieved. The acceleration of a soliton by interaction with the dispersive wave (see the CDE curve in Fig. 1) is directly related to the strength of the induced frequency shift and to the profile of the group index $n_g = c\beta'(\omega)$, which is shown in Fig. 3(a). The GVD parameter $\beta_2 = \beta''(\omega)$changes together with the soliton frequency. For the presented set-up β_2 decreases in absolute value [see the vertical dashed lines in Fig. 2(a) and (c)]. An

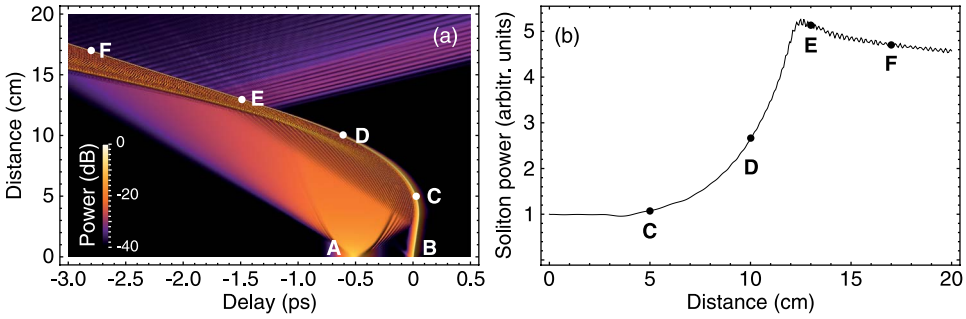

Fig. 1. Interaction of a broadened dispersive wave packet (A) with the velocity matched soliton (B), which slightly perturbs fiber's refraction index [see (2) for parameters]. The interaction is referred to as collision. It is accompanied by scattering, i.e., reflection and transmission of the dispersive wave. (C–E) The wave packet is nearly perfectly reflected in the moving frame. In the laboratory frame, both the initial and the reflected dispersive waves move in the same direction. The soliton experiences frequency shift, which leads to soliton compression and acceleration. The latter manifests itself via the curved soliton trajectory. (E and F) Frequency-shifted soliton is no longer velocity matched to the dispersive wave. The soliton is then to some extent transparent for the dispersive wave and moves with the nearly constant velocity. (Left) Space–time plot of the power density. (Right) Soliton peak power versus propagation distance.

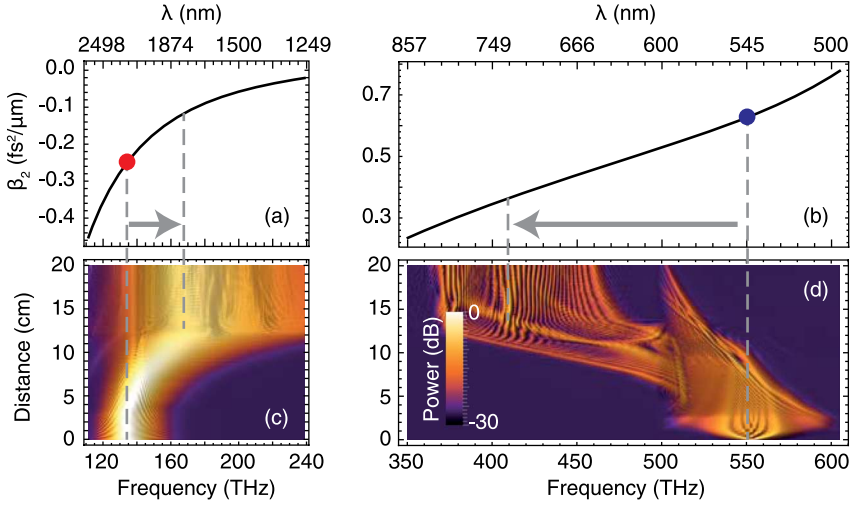

Fig. 2. Collision process between a controlling dispersive wave and a soliton in the spectral domain [see (2) for parameters]. (a) GVD β_2 profile in the anomalous dispersion regime over the range of the induced soliton frequency shift. (b) The same over the frequency conversion range of the dispersive wave. (c) and (d) Evolution of spectra along the fiber in the range of the soliton (c) and the dispersive wave (d). The dashed gray lines mark the input and output center frequencies of the soliton and the dispersive wave. The red and blue dots correspond to the initial center frequency of the soliton and dispersive wave, respectively.

efficient pulse manipulation, like that in Fig. 1(b), requires a sharp variation of β_2 along the induced soliton frequency shift [see the left branch in Fig. 3(a)].

As the soliton experiences frequency shift toward the lower GVD values, it is adiabatically compressed similarly to the compression in prefabricated dispersion decreasing fibers [37]. In our case, the frequency shift is controlled by interaction with dispersive waves. The resulting compression factor is related to the strength of the induced frequency shift: lower GVD values lead to higher peak intensities and to lower pulse width. For a steep GVD profile, a relatively small frequency shift may already result in strong compression. In the above example, the steepness precondition is fulfilled due to the vicinity of vibrational resonances. Simulations

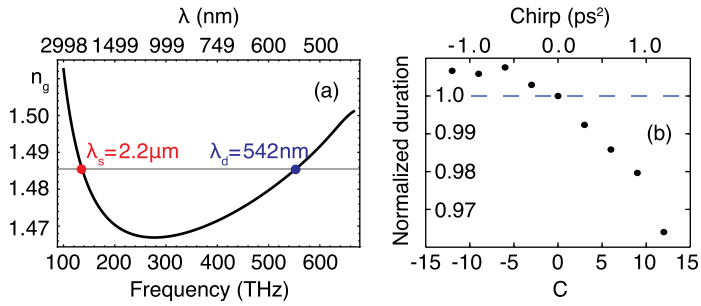

Fig. 3. (a) Group index n_g of the ESM fiber [35]. Positions of the soliton and dispersive wave are indicated by the red and blue dots, respectively. (b) Pulse duration at the fiber output (30 cm) is shown in dependence on the dispersive wave chirp C (the duration is normalized to pulse duration for $C = 0$). Here, $t_d = 300$ fs, and $\mathcal{E}_{d0} = 0.3\mathcal{E}_{s0}$; the other parameters are as in (2).

shown in Figs. 1 and 2 demonstrate an adiabatic-like compression away from the limitations that were observed in the system discussed above. Note, that soliton compression [see Figs. 1(b) and 2(c)] mainly takes place in a short interval between 7 and 12 cm of the propagation length. One can then conclude, that the "slower" phenomena such as attenuation and Raman self-frequency shift might require a more careful preparation of the initial pulses, but cannot destroy the compression as such.

3. Effect of Chirp on Soliton Compression and Acceleration

The instantaneous frequency, which can change along the dispersive pulse, has impact on group-velocity matching condition just because upon propagation the frequency-shifted soliton interacts with different portions of the dispersive wave. This fact suggests use of the chirp as an additional control parameter here. A carefully chosen chirp avoids early stagnation of the scattering process due to the varying soliton frequency. As the latter constantly increases during the soliton compression process, the frequency of the dispersive wave should constantly decrease [see Fig. 3(a)], such that a positive chirp has to be induced.

To illustrate the chirp effect, we choose a dispersive pulse with $t_d = 300$ fs and $\mathcal{E}_{d0} = 0.3\mathcal{E}_{s0}$. The other parameters are as in (2). With this setup, we performed several simulations at different chirp parameters varying from $C = -12$ to 12. Scattering of the dispersive wave on the soliton is shown in Fig. 4(a)–(h) for a reference value $C = 0$ and an exemplary $C = 6$ $(\text{GDD} \approx 1620\ \text{fs}^2)$.

The most pronounced effect of a positively chirped dispersive wave is a stronger acceleration of the soliton, that is, the soliton arrives earlier at the fiber end [compare Fig. 4(c) and (d)]. Soliton compression is slightly improved [compare Fig. 4(a) and (b)]. The compression factor for different values of C is shown in Fig. 3(b). As expected, the positive chirp enhances the compression factor, as compared to the $C = 0$ case, however, the improvement is limited by several percents. Another feature is that a positive chirp makes the spectrum of the dispersive wave broader, both at the beginning of the fiber and after scattering on the soliton [compare Fig. 4(e), (g) and (f), (h)].

For a negative chirp, the spectrum of the dispersive wave initially appears broadened, this initial stage is followed by spectral narrowing after a certain distance (not shown). In turn, this leads to deterioration of the group velocity matching condition resulting in a less pronounced soliton acceleration. At further increase or decrease of the initial chirp, temporal reshaping of the dispersive wave becomes dominant. This situation is considered in the next section.

4. Effect of Strongly Chirped Dispersive Waves on the Collision Process

In this section we focus on a situation previously reported in [23], which enables practically ideal pulse compression to a single-cycle soliton. Specifically, we consider two sets of parameters for

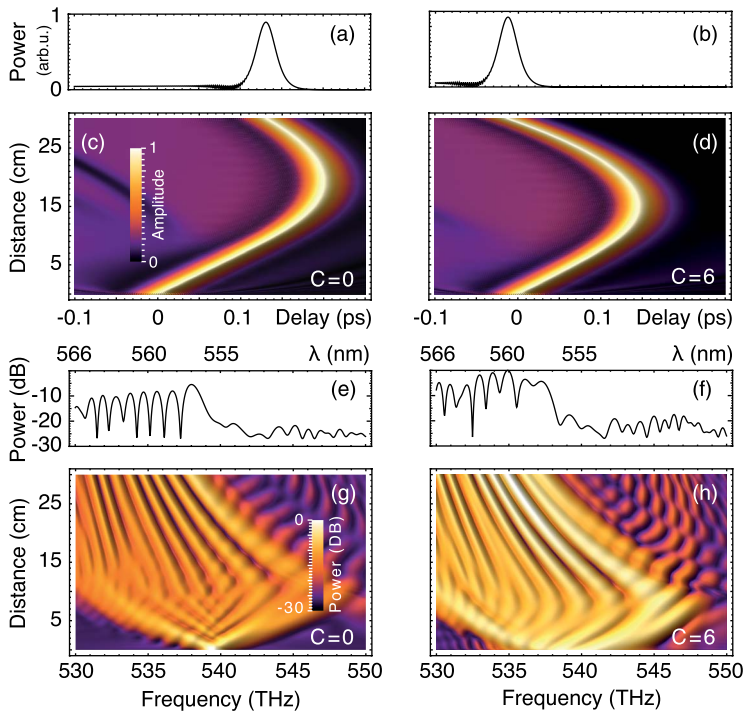

Fig. 4. Evolution of a soliton interacting with the unchirped ($C = 0$, left column) and chirped ($C = 6$, right column) dispersive wave. (a) and (b) Output pulses at $z = 30$ cm. (c) and (d) Space–time evolution. (e) and (f) Output spectrum of the dispersive wave. (g) and (h) Dispersive wave spectrum along the fiber. Soliton spectrum (not shown) behaves similar to that on Fig. 2(c). Here, $t_d = 300$ fs and $\mathcal{E}_{d0} = 0.3\mathcal{E}_{s0}$, and the other parameters are as in (2).

the dispersive wave packets with two different widths

$$t_0 = 300\,\text{fs}, \quad t_d = 100\,\text{fs}, \quad \mathcal{E}_{d0} = 0.6\mathcal{E}_{s0} \tag{3}$$

$$t_0 = 500\,\text{fs}, \quad t_d = 300\,\text{fs}, \quad \mathcal{E}_{d0} = 0.4\mathcal{E}_{s0} \tag{4}$$

and the other parameters are as in (2). The parameters are selected to show the main features of the chirped dispersive wave action, which are in general rather robust and do not depend on the particular parameter set. Fig. 5(a) and (d) depicts the corresponding evolution in the time domain for $C = 0$. We now repeat these calculations applying an initial chirp $C = \pm 40$ (GDD $\approx \pm 250$ fs^2) to the dispersive wave. The latter starts to behave in a different manner both prior and upon the contact with the soliton. We stress that the regimes that are shown in Fig. 5(a) and (d) already provide nearly the shortest compressed soliton. Therefore, one cannot improve the compression factor by using chirp. One can, however, change soliton's trajectory and control its delay at the end of the fiber. This possibility is investigated in this section. Another option arises when some perturbations, such as Raman effect, disrupt the optimal compression. One can try to restore the ideal situation by imposing a proper chirp. This possibility is investigated in the next section.

Fig. 5(b) and (e) depicts effect of the positive chirp $C = 40$ that enhances the initial temporal broadening of the dispersive wave. Consequently, the scattering on the soliton occurs earlier in the propagation and the soliton is affected by a temporally wider pulse. Soliton acceleration is therefore more pronounced, and the induced delay in Fig. 5(b) and (e) is considerably larger than that from the reference calculation in Fig. 5(a) and (d).

Fig. 5(c) and (f) depicts effect of the negative chirp $C = -40$, the dispersive wave is now compressed until its chirp is compensated. Thereafter, the dispersive wave behaves similarly to the

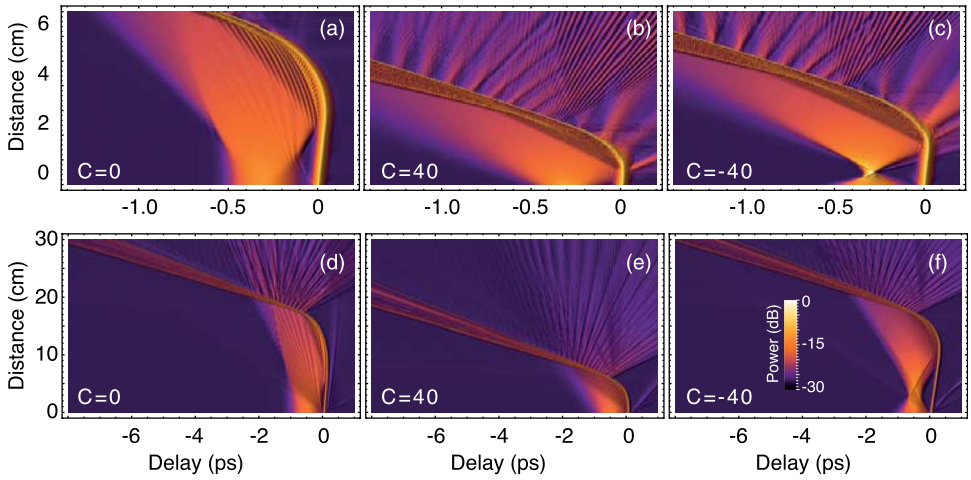

Fig. 5. Temporal dynamics of scattering of dispersive waves with different input chirps on a group velocity matched soliton. The dispersive wave parameters are given by (3) for (a)–(c) and by (4) for (d)–(f). The other parameters are as in (2).

case with the initially positive chirp. Soliton acceleration may be either less or more pronounced than that in the reference calculation. The more pronounced acceleration occurs if prior to the collision the chirped pulse manages to become temporally wider than the unchirped one in the reference calculation [see Fig. 5(c), as opposed by Fig. 5(f)]. Note also that amplitude of a negatively chirped pulse is, at least for a while, larger than that of the unchirped one. Upon collision this property of the dispersive pulse may significantly affect the soliton.

Peak power of the compressed solitons and several field snapshots are shown in Fig. 6. Here the right column is for the parameters from (3) [see the first row in Fig. 5], the left column is for (4) [the second row in Fig. 5]. The other parameters are as in (2). We show the reference calculation for $C = 0$ and two calculations for $C = \pm 40$. In all cases, the soliton is abruptly compressed to a nearly single-cycle state, after which it slowly degenerates into a state with lower peak intensity and broader pulse width in a full analogy with Fig. 1(b).

As expected, the imposed chirp cannot improve the almost perfect compression factor: the maximum intensity is nearly the same for all three calculations in Fig. 6(a) and for those in Fig. 6(b). Both maximum intensities correspond to a nearly single-cycle pulse. However, one can control the exact position at which the most compressed soliton appears. Positive chirps shift the position of the maximal compression to lower values of z, negative chirps work in both directions. Snapshots of the soliton field and the surrounding dispersive waves at different stages of propagation are shown in Fig. 6(c)–(h). In all cases, we receive a cycle number less than 2 at the end of the fiber. Here the cycle number has been calculated using a full width at half maximum of the soliton intensity profile.

In summary, exploiting temporal reshaping, a strong initial chirp can be used as an alternative way to adjust both the dispersive wave duration and the time delay. The chirp can be used to adapt the compression behavior to the available length of the fiber [see Fig. 6(e)]. It is noteworthy that the nonlinear effects discussed in the previous section indicate that introducing a chirp to a dispersive wave is not completely equivalent to changing the delay between the soliton and the dispersive wave.

5. Chirped Dispersive Waves for Cancellation of the Raman Soliton Self-Frequency Shift

So far, we have excluded the Raman effect in our considerations. The Raman effect is responsible for the soliton self-frequency shift, and the latter terminates the velocity matching condition

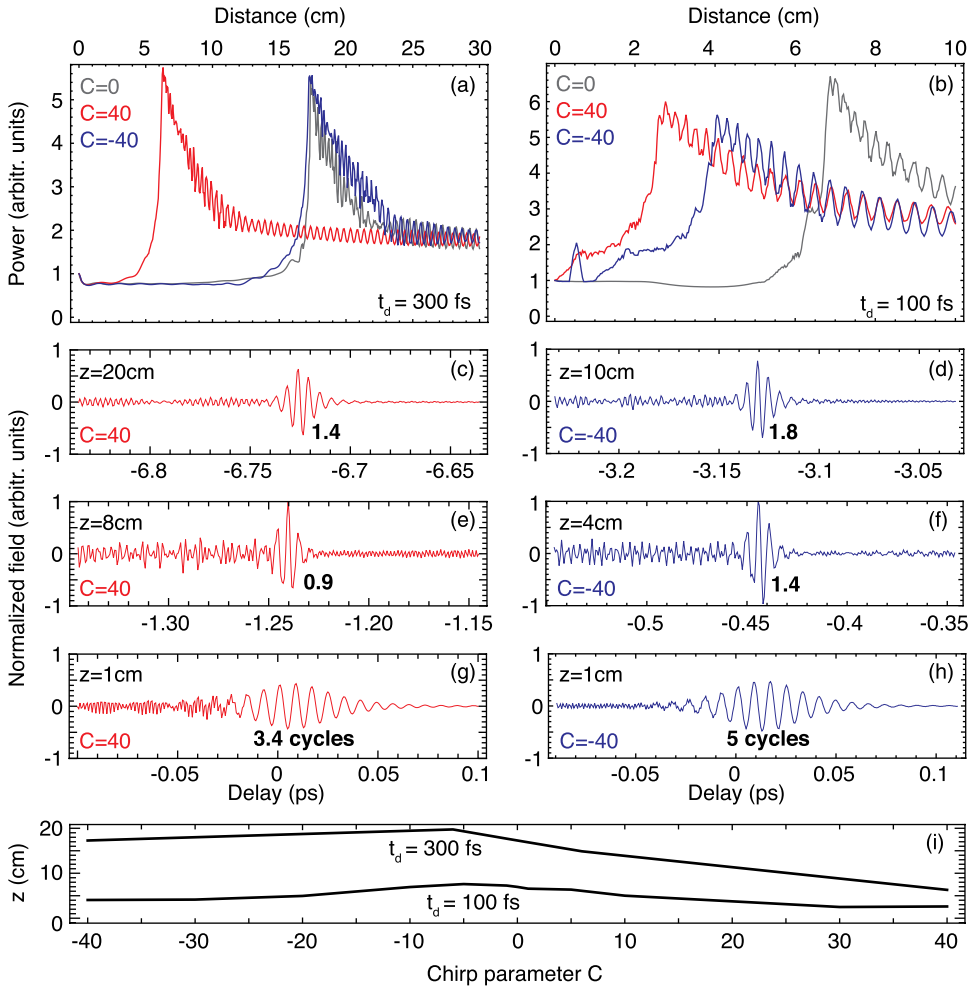

Fig. 6. (a) and (b) Evolution of the soliton peak power with z and (c)–(h) exemplary field snapshots for different input chirps C of the dispersive wave. The right column is for the parameters from (3) (also corresponds to the first row in Fig. 5), and the left column is for (4) (the second row in Fig. 5). The other parameters are as in (2). (g) and (h) The initial few-cycle fundamental soliton is abruptly compressed to (e) and (f) a single-cycle state and then slowly degenerates to (c) and (d) a two-cycle pulse. (e) With the initial chirp C, one can control the exact position z at which the shortest soliton appears.

shown in Fig. 3(a) as the soliton propagates along the fiber. As it appears, the Raman effect does not exclude the collision process and the subsequent soliton reshaping [4], [7], [12] but requires a more careful selection of the initial pulse parameters [38], [39]. For instance, one may start with a blue-shifted soliton such that it is pushed to the velocity-matched state by the soliton self-frequency shift. Alternatively, one can shift the initial frequency of the dispersive wave, to ensure velocity matching upon collision with the soliton. In both cases, as opposed to the Raman-free situation, the initial velocities of both pulses can not be not too close to each other. Another requirement is that, upon collision, the soliton frequency shift (the one that is induced by the scattered dispersive wave) should overcome the Raman self-frequency shift in order to obtain an effective soliton compression.

Fig. 7 shows interaction of the dispersive wave with the soliton under the influence of the Raman effect. We use the following parameters of the dispersive wave:

$$t_0 = 500\,\text{fs}, \quad t_d = 62.5\,\text{fs}, \quad \mathcal{E}_{d0} = 0.67\mathcal{E}_{s0}. \tag{5}$$

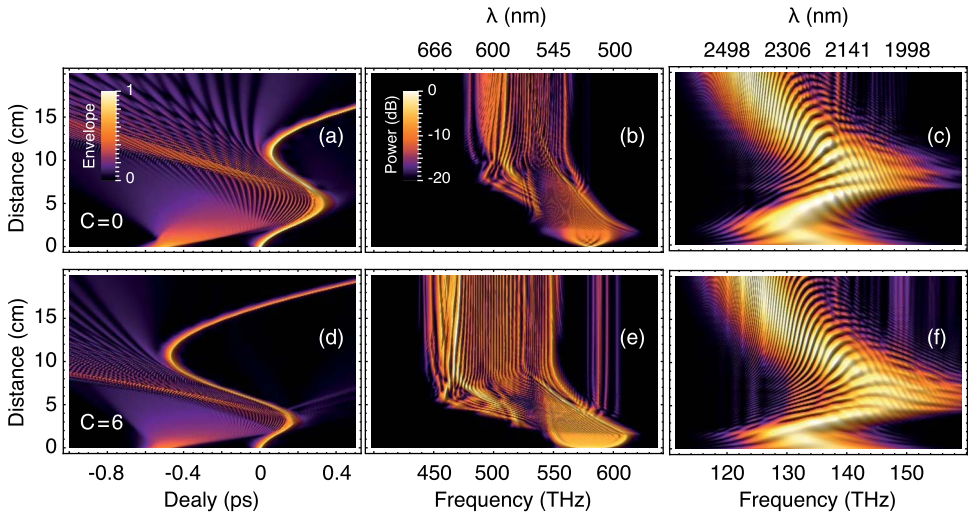

Fig. 7. Dynamics of soliton and dispersive wave interaction taking into account the Raman process. (a) and (b) Temporal domain. (b) and (e) Spectral domain of the dispersive wave. (c) and (f) Spectral domain of the soliton. The first row is a reference calculation with $C = 0$, and the second row is for $C = 6$ (GDD ≈ 1620 fs^2) (d)–(f). Other parameters are given in (5) for the dispersive wave and in (2) for the soliton.

Note that frequency of the dispersive wave is shifted, as compared to (2) and Fig. 3(a); the shift was selected to compensate the self-frequency-shift of the soliton.

In the first place, the soliton self-frequency shift is clearly canceled as long as the collision takes place, independently of the chirp. Note that as discussed above, the soliton efficiently interacts with the extended low-level background created by the broadening of the dispersive pulse. At higher intensities the dispersive wave mostly crosses the soliton, with only a small interacting part remaining. In the presence of the Raman effect, intensity of the background must be small but not too small, in order to compensate for the self-frequency shift. Still, at a certain point, the interaction ceases to compensate the Raman effect and the latter resumes control over the soliton trajectory. In contrast to the Raman-free case, an adjusted interaction length is now essential for the formation of a compressed soliton at the fiber output.

The presence of the chirp may serve to enhance the interaction length, leading to a stronger compression of the soliton. This is exemplified in Fig. 8(a) and (b), where the behavior of the soliton maximum is shown for different chirp factors as well as for different amplitudes of the dispersive wave. Obviously, in the presence of Raman effect, the compression factor due to interaction with the dispersive wave is less than in the case without Raman. For low amplitudes of the dispersive wave, even a simple re-compression may be impossible to achieve. Nevertheless, the presence of a chirp in the dispersive wave can improve the situation [see Fig. 8(c)]. One can see, that, although the presence of the chirp improves the compression, the improvement is relatively small. Nevertheless, it can be almost one order of magnitude higher than for the case when the Raman effect is neglected. Besides, the comparison of Fig. 7(b) and (e) shows that the spectral dynamics of the dispersive wave is significantly different in the case with and without chirp. In particular, a low-frequency part of the dispersive wave appears much more pronounced in the case with chirp. This clearly shows once more that the (linear) temporal reshaping of the dispersive wave plays only a minor role in this case. Much more important is the fact that spectral resonance relations between the soliton and dispersive wave are modified by the chirp. This is further corroborated by Fig. 9, which shows XFROG trace directly after the interaction (at $z =$ 10 cm for the Fig. 7). The strong "vertical line" in the center is responsible for the soliton whereas the side lobes show the dispersive wave. One can see that the interaction with the chirped dispersive wave, in comparison to the interaction with a wave without chirp, strongly modifies the dispersive wave itself, as well as the low-frequency part of the "solitonic part."

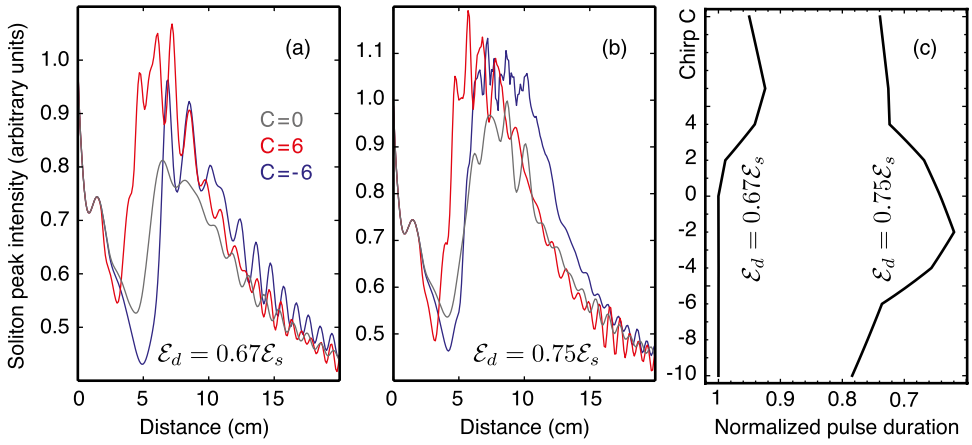

Fig. 8. (a) and (b) Evolution of the soliton maximum with z for $\mathcal{E}_d = 0.67\mathcal{E}_s$ (a) and $\mathcal{E}_d = 0.75\mathcal{E}_s$ (b). The color-coded lines specify values of the input chirp parameter C of the dispersive wave. The other parameters as in (5) for the dispersive wave and in (2) for the soliton. (c) The minimal soliton duration normalized by the initial duration versus the chirp parameter C.

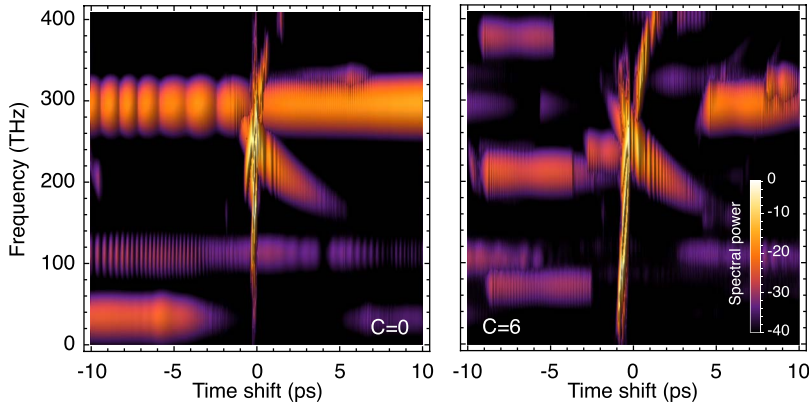

Fig. 9. XFROG representation of the dispersive wave that is scattered by a fundamental soliton in the presence of the Raman self-frequency shift. We use the parameters of Fig. 8 and take $z = 10$ cm. (a) $C = 0$, and (b) $C = 6$.

6. Conclusion

In conclusion, we have studied the dynamics of a short soliton resonantly interacting with a chirped dispersive wave packet in an ESM photonic crystal fiber. We found that a relatively small chirp can already significantly modify the dynamics of the interaction process. In general, there are two major mechanisms influencing the dynamics, namely, one related to the frequency-matching condition (since as the frequency of soliton changes, frequency of the dispersive wave must be also changed to keep the interaction working) and a second one relating to purely linear reshaping of the chirped dispersive wave in time. The latter mechanism is important for large input chirps and allows controlling the point where dispersive wave and soliton start to interact. On the other hand, the former case allows for an improvement of the soliton-dispersive wave interaction. These two mechanisms enable a match of the compression behavior to the fiber length. Specifically, one can obtain the maximum soliton compression at shorter propagation distances. Moreover, the chirped dispersive wave is very useful for the control of the soliton dynamics in presence of the Raman effect, allowing to partially compensate the Raman-induced soliton frequency shift. The soliton compression degree can also be improved by introducing a chirp into

the dispersive wave, although this improvement is rather moderate (up to approximately 10%). Although all reasonable values of chirp has been scanned in search for the best compression, the whole parameter range is too large to come to the definite conclusion about the best possible compression. In general, the chirp in the dispersive wave does provide an additional independent degree of freedom, enabling the modification of time and position of the first collision. In particular, introduction of a positive chirp reduces this time and provides longer interaction distances. The outlined mechanisms enable substantial adaption of the adiabatic soliton compression to a given dispersion characteristics of the fiber.

References

[1] T. Balciunas *et al.*, "A strong-field driver in the single-cycle regime based on self-compression in a Kagome fibre," *Nature Commun.*, vol. 6, no. 6117, p. 6117, Jan. 2015.
[2] A. Demircan, S. Amiranashvili, and G. Steinmeyer, "Controlling light by light with an optical event horizon," *Phys. Rev. Lett.*, vol. 106, no. 16, Apr. 2011, Art. no. 163901.
[3] D. V. Skryabin and A. V. Gorbach, "Colloquium: Looking at a soliton through the prism of optical supercontinuum," *Rev. Modern Phys.*, vol. 82, no. 2, pp. 1287–1299, Apr.–Jun. 2010.
[4] A. V. Gorbach and D. V. Skryabin, "Bouncing of a dispersive pulse on an accelerating soliton and stepwise frequency conversion in optical fibers," *Opt. Exp.*, vol. 15, no. 22, Oct. 2007, Art. no. 14560.
[5] A. V. Yulin, D. V. Skryabin, and P. S. J. Russell, "Four-wave mixing of linear waves and solitons in fibers with higher-order dispersion," *Opt. Lett.*, vol. 29, no. 20, pp. 2411–2413, Oct. 2004.
[6] C. M. De Sterke, "Optical push broom," *Opt. Lett.*, vol. 17, no. 13, pp. 914–916, 1992.
[7] T. G. Philbin *et al.*, "Fiber-optical analog of the event horizon," *Science*, vol. 319, no. 5868, pp. 1367–1370, 2008.
[8] D. Faccio, "Laser pulse analogues for gravity and analogue hawking radiation," *Contemporary Phys.*, vol. 53, no. 2, pp. 97–112, 2012.
[9] R. Smith, "The reflection of short gravity waves on a non-uniform current," *Math. Proc. Camb. Phil. Soc.*, vol. 78, no. 3, pp. 517–525, Nov. 1975.
[10] R. Driben, F. Mitschke, and N. Zhavoronkov, "Cascaded interactions between Raman induced solitons and dispersive waves in photonic crystal fibers at the advanced stage of supercontinuum generation," *Opt. Exp.*, vol. 18, no. 25, pp. 25993–25998, Dec. 2010.
[11] A. Demircan *et al.*, "Rogue events in the group velocity horizon," *Sci. Rep.*, vol. 2, p. 850, Nov. 2012.
[12] A. Demircan, S. Amiranashvili, C. Brée, C. Mahnke, F. Mitschke, and G. Steinmeyer, "Rogue wave formation by accelerated solitons at an optical event horizon," *Appl. Phys. B*, vol. 115, no. 3, pp. 343–354, Aug. 2014.
[13] I. Oreshnikov, R. Driben, and A. V. Yulin, "Interaction of high-order solitons with external dispersive waves," *Opt. Lett.*, vol. 40, no. 23, pp. 5554–5557, Dec. 2015.
[14] I. Oreshnikov, R. Driben, and A. V. Yulin, "Weak and strong interactions between dark solitons and dispersive waves," *Opt. Lett.*, vol. 40, no. 21, pp. 4871–4874, Nov. 2015.
[15] K. E. Webb *et al.*, "Nonlinear optics of fibre event horizons," *Nature Commun.*, vol. 5, no. 4969, Sep. 2014.
[16] N. G. R. Broderick, D. Taverner, D. J. Richardson, M. Ibsen, and R. I. Laming, "Optical pulse compression in fiber Bragg gratings," *Phys. Rev. Lett.*, vol. 79, no. 23, pp. 4566–4569, Dec. 1997.
[17] M. Wimmer *et al.*, "Optical diametric drive acceleration through action-reaction symmetry breaking," *Nature Phys.*, vol. 9, no. 12, pp. 780–784, 2013.
[18] L. Tartara, "Frequency shifting of femtosecond pulses by reflection at solitons," *IEEE J. Quantum Electron.*, vol. 48, no. 11, pp. 1439–1442, Aug. 2012.
[19] R. Driben and I. Babushkin, "Accelerated rogue waves generated by soliton fusion at the advanced stage of supercontinuum formation in photonic-crystal fibers," *Opt. Lett.*, vol. 37, no. 24, pp. 5157–5159, Dec. 2012.
[20] R. Driben, A. V. Yulin, A. Efimov, and B. A. Malomed, "Trapping of light in solitonic cavities and its role in the supercontinuum generation," *Opt. Exp.*, vol. 21, no. 16, pp. 19091–19096, Aug. 2013.
[21] A. V. Yulin, R. Driben, B. A. Malomed, and D. V. Skryabin, "Soliton interaction mediated by cascaded four wave mixing with dispersive waves," *Opt. Exp.*, vol. 21, no. 12, pp. 14481–14486, Jun. 2013.
[22] S. Batz and U. Peschel, "Diametrically driven self-accelerating pulses in a photonic crystal fiber," *Phys. Rev. Lett.*, vol. 110, no. 19, May 2013, Art. no. 193901.
[23] A. Demircan, S. Amiranashvili, C. Brée, U. Morgner, and G. Steinmeyer, "Adjustable pulse compression scheme for generation of few-cycle pulses in the midinfrared," *Opt. Lett.*, vol. 39, no. 9, pp. 2735–2738, May 2014.
[24] L. Tartara, "Soliton control by a weak dispersive pulse," *J. Opt. Soc. Amer. B, Opt. Phys.*, vol. 32, no. 3, p. 395, Mar. 2015.
[25] D. Gabor, "Theory of communication," *J. Inst. Elect. Eng.*, vol. 93, no. 3, pp. 429–457, 1946.
[26] M. Born and E. Wolf, *Principles of Optics*, 7th ed. Cambridge, MA, USA: Cambridge Univ. Press, 1999.
[27] S. Amiranashvili and A. Demircan, "Hamiltonian structure of propagation equations for ultrashort optical pulses," *Phys. Rev. A*, vol. 82, no. 1, Jul. 2010, Art. no. 013812.
[28] R. W. Boyd, *Nonlinear Optics*, 3rd ed. New York, NY, USA: Academic, 2008.
[29] M. Kolesik, J. V. Moloney, and M. Mlejnek, "Unidirectional optical pulse propagation equation," *Phys. Rev. Lett.*, vol. 89, no. 28, Dec. 2002, Art. no. 283902.
[30] M. Kolesik and J. V. Moloney, "Nonlinear optical pulse propagation simulation: From Maxwell's to unidirectional equations," *Phys. Rev. E, Stat. Phys. Plasmas Fluids Relat. Interdiscip. Top.*, vol. 70, no. 3, 2004, Art. no. 036604.

[31] A. V. Husakou and J. Herrmann, "Supercontinuum generation of higher-order solitons by fission in photonic crystal fibers," *Phys. Rev. Lett.*, vol. 87, no. 20, 2001, Art. no. 203901.
[32] A. Husakou, "Nonlinear phenomena of ultrabroadband radiation in photonic crystal fibers and hollow waveguides," Ph.D. dissertation, Physical Dept., Freie Univ. Berlin, Berlin, Germany, 2002.
[33] I. Babushkin and J. Herrmann, "High energy sub-10 fs pulse generation in vacuum ultraviolet using chirped four wave mixing in hollow waveguides," *Opt. Exp.*, vol. 16, no. 22, pp. 17774–17779, Oct. 2008.
[34] I. V. Babushkin, F. Noack, and J. Herrmann, "Generation of sub-5 fs pulses in vacuum ultraviolet using four-wave frequency mixing in hollow waveguides," *Opt. Lett.*, vol. 33, no. 9, pp. 938–940, May 2008.
[35] J. M. Stone and J. C. Knight, "Visibly white light generation in uniform photonic crystal fiber using a microchip laser," *Opt. Exp.*, vol. 16, no. 4, pp. 2670–2675, Feb. 2008.
[36] C. Agger *et al.*, "Supercontinuum generation in ZBLAN fibers-detailed comparison between measurement and simulation," *J. Opt. Soc. Amer. B, Opt. Phys.*, vol. 29, no. 4, pp. 635–645, Apr. 2012.
[37] S. V. Chernikov, D. J. Richardson, D. N. Payne, and E. M. Dianov, "Soliton pulse compression in dispersion-decreasing fiber," *Opt. Lett.*, vol. 18, no. 7, pp. 476–478, Apr. 1993.
[38] A. Demircan, S. Amiranashvili, C. Brée, and G. Steinmeyer, "Compressible octave spanning supercontinuum generation by two-pulse collisions," *Phys. Rev. Lett.*, vol. 110, no. 23, Jun. 2013, Art. no. 233901.
[39] A. Demircan, S. Amiranashvili, C. Brée, U. Morgner, and G. Steinmeyer, "Supercontinuum generation by multiple scatterings at a group velocity horizon," *Opt. Exp.*, vol. 22, no. 4, pp. 3866–3879, Feb. 2014.